Contribution from the Department of Chemistry,
Iowa State University, Ames, Iowa 50011

Condensed Metal Cluster Iodides Centered by Noble Metals. Six Examples of Cubic R_3I_3Z Phases (R = La, Pr; Z = Os, Ir, Pt)

Peter K. Dorhout, Martin W. Payne, and John D. Corbett*

Received June 21, 1991

The isostructural compounds R_3I_3Z (R = La, Pr; Z = Os, Ir, Pt) are synthesized by reaction of R turnings, RI_3, and powdered Z at ~950 °C in sealed Nb containers. Neighboring Z elements or lower temperatures produce other cluster compounds. The structure of Pr_3I_3Pt was refined and shown to be isostructural with Ca_3PI_3 (and Gd_3Cl_3C): $I4_132$, $Z = 12$, $a = 12.4150$ (4) Å, $R/R_w = 2.6/4.4\%$. Platinum-centered Pr_6I_{12}-type clusters share three nonadjacent Pr-Pr edges to give 4_1 cluster chains in a defect NaCl arrangement: $Pr_{6/2}(Pt)I_{12/4}$. Magnetic and resistivity data suggest the phases are poor metals.

Introduction

The bountiful chemistry of reduced rate-earth-metal (R) halides is yielding a growing harvest of unusual compounds. Many of these are structurally composed of basic building blocks of centered R-metal octahedra that are edge-bridged by iodine atoms, $R_6I_{12}Z$, where Z is the centered or interstitial element. These basic units occur in three different types of structures: halogen-bridged networks of isolated clusters in $R_6I_{10}Z$[1] and $R_7I_{12}Z$[2,3] phases, with Z being many of the noble metals or their neighbors, condensed edge-sharing arrays of quasi-infinite single chains in Y_4I_5C,[4] Gd_4I_5Si,[5] or Pr_4I_5Ru,[6] for example, or with further condensation to give double chain compounds as found in $Y_6I_7C_2$[4] or Pr_3I_3Ru.[7] An alternative condensation into a three-dimensional, defect-NaCl structure (Ca_3PI_3-type[8]) has been reported for Gd_3Cl_3C[9] and, more recently, for Gd_3I_3Si.[5] The present article reports the discovery of several noble-metal-centered R_3I_3Z examples with the same cubic structure for R = La and Pr but with encapsulation of the heavy platinum metals Os, Ir, or Pt. These phases should be distinguished from monoclinic R_3I_3Z double-chain compounds that occur for Z = Ru and R = La, Pr, Gd, Y, and Er and for Z = Ir with R = Gd and Y but not (so far) R = La and Pr.[7]

Experimental Section

Synthesis. The rare-earth metals used, the preparation and purification techniques for their triiodides, the origin and purities of the interstitial reagents, reaction techniques in welded Nb tubing, and the Guinier X-ray powder pattern methods have all been described before.[1-3] The syntheses of the black R_3I_3Z phases employed stoichiometric proportions of La or Pr turnings, the corresponding RI_3, and powdered elemental Z for periods of 23-35 days. About 5% ROI and 5% RI_x ($2.0 \le x \le 2.5$) were common contaminants at the temperatures employed.

As with the R_4I_5Z syntheses described earlier,[6] the stabilities of these particular Pr_3I_3Z phases also appear to be quite temperature dependent. Between 800 and 900 °C $Pr_6I_{10}Z$ and $Pr_7I_{12}Z$ dominate the product mixtures with generally less than 50% yields of the cubic Pr_3I_3Z (Z = Os, Ir, Pt). Higher temperatures, 950-975 °C, afford high yields (>80%) of the phases of interest although in the case of Pr_3I_3Os the compounds $Pr_6I_{10}Os$ and Pr_4I_5Os still constitute a major share of the product.

Reactions with R = La afford less complicated product mixtures although they too display a temperature dependence. For Z = Os and Ir, La_3I_3Z forms between 900 and 975 °C, whereas at 800-850 °C, $La_7I_{12}Z$ is the major phase. For Z = Pt, an as yet unidentified phase competes at higher temperatures (975 °C) with La_3I_3Pt. Small amounts of LaI_2 are commonly produced under all of these conditions as well. All of the compounds are moisture sensitive and react with air to form brown liquids. The Guinier-based lattice constants of the new R_3I_3Z phases are given in Table I.

Table I. Lattice Parameters for the Cubic R_3I_3Z Phases (R = La, Pr; Z = Os, Ir, Pt)

compd	a,[a] Å	compd	a,[a] Å
La_3I_3Os	12.7003 (5)	Pr_3I_3Os[b]	12.503 (8)
La_3I_3Ir	12.5770 (6)	Pr_3I_3Ir	12.3816 (4)
La_3I_3Pt	12.6204 (4)	Pr_3I_3Pt	12.4150 (4)

[a] Based on Guinier powder diffraction at room temperature with Si as an internal standard, $\lambda = 1.540562$ Å. [b] Obtained only in small amounts.

Table II. Some Collection and Refinement Data for Pr_3I_3Pt

space group; Z	$I4_132$ (No. 214); 12	no. of unique data with $F_o^2 > 3\sigma(F_o^2)$	544
V,[a] Å^3	1913.55 (5)		
μ(Mo Kα), cm^{-1}	591.6	params refined	14
transm coeff range	0.52-1.00	R,[b] %	2.6
		R_w,[c] %	4.4

[a] Lattice dimension in Table I. [b] $R = \sum||F_o| - |F_c||/\sum|F_o|$. [c] $R_w = [\sum w(|F_o| - |F_c|)^2/\sum w(F_o)^2]^{1/2}$; $w = [\sigma(F)]^{-2}$.

Table III. Positional and Isotropic Equivalent Thermal Parameters for Pr_3I_3Pt, Space Group $I4_132$

atom	x	y	z	B_{iso}, Å^2
Pt	1/8	1/8	1/8	0.5803 (2)
Pr	1/8	0.10666 (6)	0.3567	0.83 (2)
I	1/8	0.38612 (7)	-0.1361	1.11 (2)

Negative results were obtained for R = La and Pr with Z = Re, Au, Ru, Rh, and Ag. Although trace quantities of (cubic) Pr_3I_3Re or La_3I_3Rh appeared to be present after reactions at 950 °C, these phases could not be isolated or positively identified with X-ray powder diffraction methods. Reactions with R = Gd yielded only the isolated cluster phase $Gd_7I_{12}Z$ for Z = Au and a new phase Gd_4I_4Z for Z = Os, Ir, and Pt.[10]

Crystallography. A parallelepiped crystal 0.5 × 0.3 × 0.3 mm chosen for the diffraction study was taken from a reaction loaded as Pr_3I_3Pt that yielded 80% of the desired product, the rest being PrOI. All measurements were made on a Rigaku AFC6R diffractometer with graphite-monochromated Mo Kα radiation from a 12-kW rotating-anode generator. Cell constants and an orientation matrix for data collection from a least-squares refinement of the setting angles of 25 centered reflections in the range $13.2 < 2\theta < 19.2$ gave a cubic cell with a dimension $a = 12.391$ Å after cell reduction. (The Guinier-based parameter, 12.4150 (4) Å, was later used for dimensional calculations.) Diffraction data were collected at 23 ± 1 °C with an ω-2θ scan and a scan rate of 16.0° min^{-1} in ω and to a limit of 65° in 2θ. Weak reflections ($I < 10\sigma(I)$) were given up to two rescans.

The space group $I4_132$ (No. 214) was uniquely determined on the basis of the systematic absences for hkl, $h + k + l \neq 2n$, and for $h00$, $h \neq 2n$. Data processing showed a negligible decay in standards, and R_{av} was 11.1% for all data in the assumed $I4_132$ space group. An empirical adsorption correction was based on the average of ψ scans of four reflections, and a correction for secondary extinction was also found to be appropriate.

Direct methods (SHELXS[11]) gave starting positions for all of the atoms in the structure. Because of the similarities in both lattice symmetry and

(1) Hughbanks, T.; Corbett, J. D. *Inorg. Chem.* **1988**, *27*, 2022.
(2) Hughbanks, T.; Corbett, J. D. *Inorg. Chem.* **1989**, *28*, 631.
(3) Payne, M. W.; Corbett, J. D. *Inorg. Chem.* **1990**, *29*, 2246.
(4) Kauzlarich, S. M.; Hughbanks, T.; Corbett, J. D.; Klavins, P.; Shelton, R. N. *Inorg. Chem.* **1988**, *27*, 1791.
(5) Nagaki, D.; Simon, A.; Borrmann, H. *J. Less-Common Met.* **1989**, *156*, 193.
(6) Payne, M. W.; Dorhout, P. K.; Corbett, J. D. *Inorg. Chem.* **1991**, *30*, 1467, 3112.
(7) Payne, M. W.; Dorhout, P. K.; Kim, S.-J.; Hughbanks, T. R.; Corbett, J. D. *Inorg. Chem.*, submitted for publication.
(8) Hamon, C.; Marchiand, R.; Laurent, Y.; Lang, J. *Bull. Soc. Fr. Miner. Crist.* **1974**, *97*, 6.
(9) Warkentin, E.; Simon, A. *Rev. Chim. Miner.* **1983**, *20*, 488.
(10) Ebihara, M.; Lachgar, A.; Corbett, J. D. To be published.
(11) Sheldrick, G. M. SHELXS-86. Institut für Anorganische Chemie, Universität Göttingen, Germany.

0020-1669/91/1330-4960$02.50/0

Table IV. Bond Distances in Pr_3I_3Pt

Pr–Pr	3.754 (2)[a]	I–I[c]	3.999 (2)
	4.0928 (8)		4.203 (1)
	4.2376 (4)[b] (×2)		
Pr–Pt	2.8851 (6) (×2)	Pt–Pt	4.4901 (6)
Pr–I	3.270 (1) (×2)		
	3.3543 (8) (×2)		

[a] Shared edges. [b] Normal to the 3-fold axis. [c] $d < 4.25$ Å.

dimensions at this point, praesodymium and iodine coordinates were assigned in parallel to those reported for Gd_3I_3Si.[5] The platinum atom inclusion followed the first least-squares cycles. The final cycle of full-matrix least-squares refinement based on 544 observed reflections ($I > 3.00\sigma(I)$) and 14 variables converged with R and R_w values of 2.6 and 4.4%, respectively, with all atoms refined anisotropically. The other enantiometer gave higher residuals. The maximum and minimum peaks remaining in the final difference Fourier map, 4.17 and −2.13 e/Å^3, were <1 Å from the Pt atom and suggested some asymmetry. Selected data for the collection and refinement are given in Table II, while atom positions and equivalent isotropic thermal parameters can be found in Table III. Bond distances are given in Table IV.

Two reflections were removed from the list of reflections before the final analysis owing to their asymmetric background. Removal of four additional reflections with $I/\sigma(I) > 5$ naturally reduced the R values, GOF, and the standard deviations of the atom parameters. However, lack of substantial, objective reasons for their removal caused us to retain them in the list.

Magnetic Susceptibility. Magnetic susceptibility measurements on several R_3I_3Z samples were performed on a Quantum Design MPMS SQUID magnetometer at fields between 1.0 and 3.0 T over the temperature range 6–300 K with a measurement every 10°. Weighed samples of 30–50 mg were sealed under <1 atm of He between two fused silica rods (3 mm o.d.) inside a fused silica tube with a similar inside diameter.

Resistivity. Measurements of the bulk resistivity of Pr_3I_3Pt were performed on 151 mg of ground and sieved powder with an average particle diameter of 200 μm that had been mixed with an equal weight of SiO_2 powder previously dried overnight in vacuo. The sample was sealed under vacuum in a Pyrex tube with an outer diameter that matched the inner diameter of the coil. The resistivity of the sample was determined from the change in Q of a high-frequency LC circuit when the sample was placed in the cavity of the coil.[12] The measurements were performed with a Q-meter (type 260A, Boonton Radio Company) at 10° intervals from 110 to 280 K.

Results and Discussion

We have previously discussed the role of transition-metal interstitial elements in the formation of $R_6I_{10}Z$[1] and $R_7I_{12}Z$[2,3] cluster phases as well as their incorporation in condensed clusters in the form of chains in R_4I_5Z.[6] Similar data on the monoclinic double-chain R_3I_3Z examples will be forthcoming.[7] Exploration of diverse noble metals as interstitials in these investigations produced several isostructural examples of a cubic phase according to X-ray powder pattern analyses (TREOR[13]), and a crystallographic study of the Pr_3I_3Pt member showed these to be isostructural with Ca_3PI_3 (as well as Gd_3Cl_3C and Gd_3I_3Si). This phase was obtained in high yields for R = La and Pr, but not for Gd, Y, or Er,[10] and occurred exclusively for Z = Os, Ir, and Pt. Temperatures of 900–975 °C (or higher) were necessary, while lower temperatures (or neighboring interstitial elements) yielded $R_6I_{10}Z$ or $R_7I_{12}Z$ cluster phases, the R_4I_5Z or monoclinic R_3I_3Z condensed chain phases, or both. Subtle stability differences and temperature-dependent equilibria are clearly involved.

The structure of these new R_3I_3Z phases can be described in terms of cubic-close-packed (ccp) I + Z layers with the R atoms ordered in 75% of the octahedral sites. Distorted trigonal antiprismatic clusters (D_3 symmetry) of praseodymium, etc. are centered by interstitial atoms (d(Pr–Pt) = 2.8851 (6) Å), and each cluster shares nonadjacent metal edges with three others in a propeller-type arrangement. Figure 1 shows such an arrangement of four clusters as viewed approximately along the 3-fold axis of the central cluster with the shared edges in heavy outline. The intervening layer of iodine and platinum and the two ccp layers of iodine only (in this region) that lie above and below the two metal layers can also be visualized. In the quantified example, the shared Pr–Pr edges are relatively short, 3.754 (2) Å, and the equilateral faces of the antiprism related by the rotation axis have the longest Pr–Pr interactions, 4.2376 (4) Å, while the unshared edges between these are intermediate, 4.093 Å. Every cluster of course lies at such a juncture of clusters. This arrangement creates a three-dimensional network of 4_1 chains of clusters as shown in Figure 2 in a cutaway of two cells and chains. The rock-salt-based cell faces are nearly edge-on on the right-hand side. All iodine in this structure is $I^{i\text{-}i\text{-}i}$ as each has four metal neighbors in a sawhorse geometry and simultaneously bridges metal–metal edges on three clusters. Three such iodines are identified by cross-hatching in Figure 1. The approximately opposed I–Pr distances are 0.08 Å longer than the others.

A somewhat different view of the cluster connectivity is shown in Figure 3, where the clusters have been replaced by single

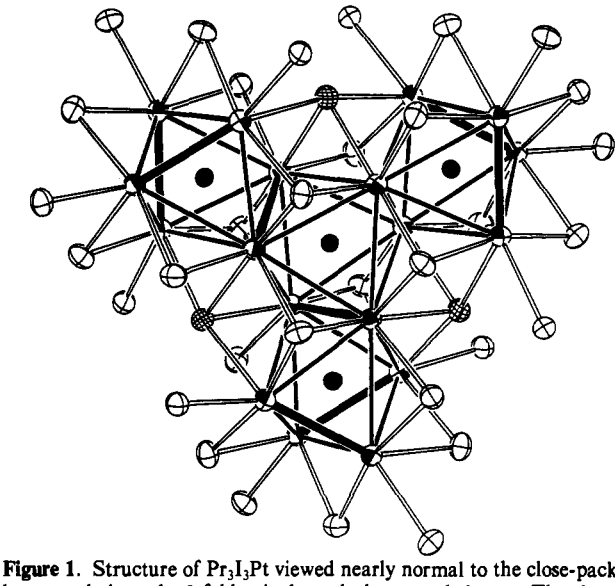

Figure 1. Structure of Pr_3I_3Pt viewed nearly normal to the close-packed layers and along the 3-fold axis through the central cluster. The clusters share Pr–Pr edges in heavy outline to produce, locally, a D_3 propeller unit. Pr atoms are shaded, I atoms are crossed, and Pt atoms are solid (98% probability) thermal ellipsoids. Three close-packed layers in this view are ordered I, I + Pt, and I, with Pr in pseudooctahedral interstices. The three iodine atoms that are crosshatched illustrate their $I^{i\text{-}i\text{-}i}$ bonding to three cluster edges.

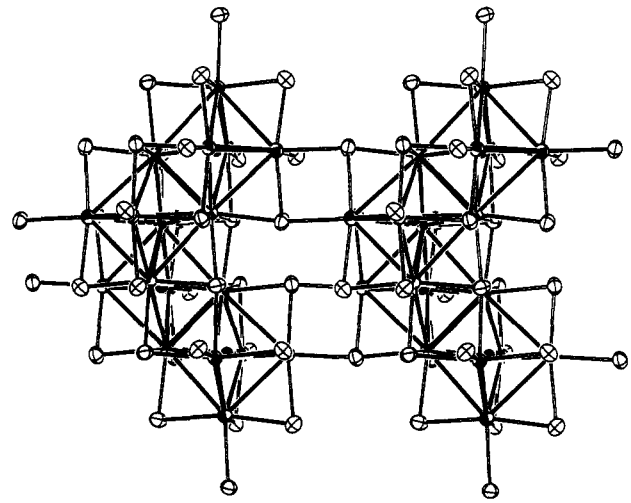

Figure 2. Section of two cells in Pr_3I_3Pt showing the 4_1 nature of cluster chains (same atom identifications as in Figure 1).

(12) Shinar, J.; Dehner, B.; Beaudry, B. J.; Peterson, D. T. *Phys. Rev. B* **1988**, *37*, 2066.

(13) Werner, P. E. TREOR-4. Trial and Error Program for Indexing of Unknown Powder Patterns. Department of Structural Chemistry, Arrhenius Laboratory, University of Stockholm, Sweden, 1984.

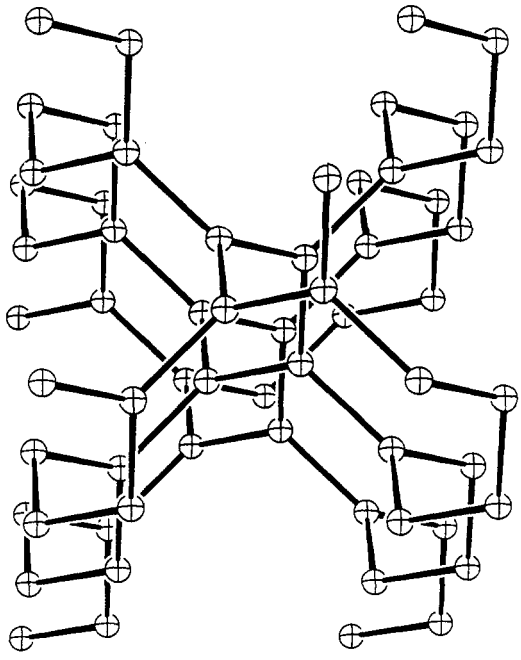

Figure 3. Overall three-dimensional character of the structure of Pr_3I_3Pt, with spheres representing the clusters and "bonds", the shared edges.

spheres, and the "bonds" represent shared edge connections between octahedra. The 4_1 chains run parallel to the three cell axes. The arrangement is systematically classified as a (10,3)-*a* net; see Wells.[14]

The transition from Gd_3I_3Si to Pr_3I_3Pt produces a somewhat larger cluster (0.07 Å in R–Z). On the other hand, there are no major changes in cluster proportions, in contrast to those found between Gd_4I_5Si and Pr_4I_5Ru chain analogues where significant π-bonding by the 4d interstitial seems responsible.[6] However, the lattice parameters listed in Table I do show an unusual trend for the series of compounds R_3I_3 (Os, Ir, Pt) for both R = La and Pr. These do not logically follow changes in metallic radii of just Z, which increase slightly over the series;[15] rather a *decrease* of 0.12 Å in the a parameter between Os and Ir is followed by a slight (0.03–0.04 Å) increase in the next step. Parallel changes but in different proportions are found in the lattice constants for the common Cu_2Mg-type structures of R_2Z for these six cases.[16] But the Pr–Pt distance in Pr_2Pt is nearly 0.3 Å larger than that in Pr_3I_3Pt. The behavior in isolated clusters is contrasting; the average Y–Z distance is substantially unchanged on going from $Y_6I_{10}Os$ to $Y_6I_{10}Ir$ although there are some changes in proportions of the centrosymmetric clusters. The Pr_3I_3Pt result represents the first time that a platinum interstitial has been characterized structurally.

The magnetic susceptibility data for Pr_3I_3Pt are shown in Figure 4 as $1/\chi$ vs T. The paramagnetic behavior follows the Curie–Weiss law (solid line) closely over the temperature range 6–300 K with a Weiss constant $\Theta = -6$ K and only slight deviations at very low temperatures. The slope yields a magnetic moment of 5.8 μ_B for Pr_3I_3Pt or 3.4 μ_B/Pr atom. This is consistent with the ideal moment of 3.58 μ_B for $4f^2$ Pr^{3+} cores and is similar to the magnetic behavior of both Pr_4I_5Ru[6] and the monoclinic Pr_3I_3Ru.[7] Coupling between lanthanide cores generally seems to be very small in these types of compounds. Susceptibility measurements on La_3I_3Ir and La_3I_3Pt both yielded temperature-independent paramagnetic signals corresponding to about 2.0×10^{-4} emu/mol after core correction, with evidence of a paramagnetic (impurity?)

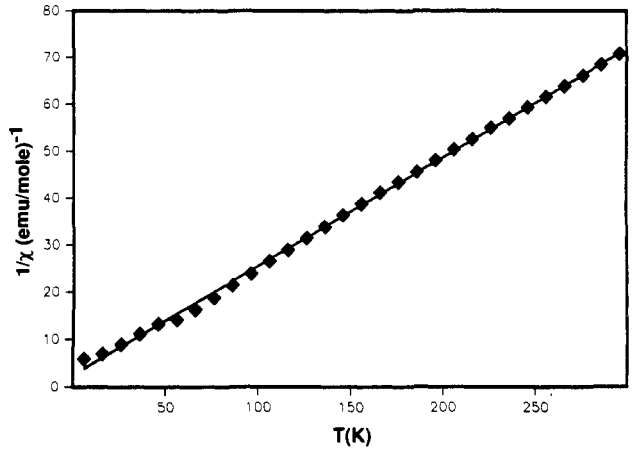

Figure 4. Inverse susceptibility as a function of temperature (K) for Pr_3I_3Pt at 3 T. The line is the Curie–Weiss fit.

tail below 20 K. This behavior parallels that of the chain compounds La_4I_5Ru[6] and $Y_6I_7C_2$[4] and suggests the R_3I_3Z compounds are probably metallic in character.

Resistivity data were obtained for Pr_3I_3Pt by means of "*Q*-factor" loss measurements. This technique was appropriate for our samples because of the combination of small crystal size and high air sensitivity. The compound showed a virtually temperature-independent resistivity between 110 and 280 K that was on the order of 0.1 Ω cm, i.e., suggestive of a poor metal. Band calculations have not been undertaken to illuminate this point. However, the conduction property is a result of subtleties in bonding near E_F that are usually quite incidental to the strong bonding at lower (more negative) energies in these compounds that is important for stability. This point has also been made by Nesper[17] in other contexts.

The occurrence of metal interstitials within rare-earth-metal clusters, microalloys of sorts, is remarkable in itself. The fact that the stability of this particular cubic R_3I_3Z phase is further limited to the three heaviest platinum metals is also noteworthy. The behavior of the corresponding 4d elements is contrasting; the versatile ruthenium gives $Pr_6I_{10}Ru$ and $Pr_7I_{12}Ru$ cluster compounds as well as the monoclinic Pr_3I_3Ru and Pr_4I_5Ru cluster chain phases, while rhodium and palladium have to date been encapsulated only in $Pr_7I_{12}Z$. Subtle factors that are not understood are clearly involved in the relative stabilities of these products. Certainly a major factor in the thermodynamic stability of these heterometallic arrays must be related to the generally high stability known for binary compounds between the electron-poor early transition metals and the electron richer late-transition-metal examples.[18] Nonetheless, our calculations on cluster halide systems with charge-consistent valence energies for the two metals have repeatedly indicated that there is only a small charge transfer between the host metal and a metal-based interstitial.[2,6,19] A large charge on Z cannot be important in determining the distortion of the clusters in Pr_3I_3Pt, contrary to a model suggested for Gd_3I_3Si.[5]

Acknowledgment. We are indebted to J. Ostenson and D. K. Finnemore for the magnetic susceptibility data and to J. Shinar for the use of the resistivity apparatus. This research was supported by the National Science Foundation, Solid State Chemistry, via Grants DMR-8318616 and -8902954 and was carried out in facilities of the Ames Laboratory, DOE.

Supplementary Material Available: Tables of data collection and refinement details and anisotropic atom displacement parameters for Pr_3I_3Pt (2 pages); a table of structure factor results for Pr_3I_3Pt (5 pages).

(14) Wells, A. F. *Three-dimensional nets and polyhedra*; J. Wiley and Sons: New York, 1977; p 35.
(15) Pearson, W. B. *The Crystal Chemistry and Physics of Metals and Alloys*; Wiley-Interscience: New York, 1972; p 151.
(16) Villars, P.; Calvert, L. D. *Pearson's Handbook of Crystallographic Data for Intermetallic Phases*, American Society of Metals: Metals Park, OH, 1985, Vol. 3.
(17) Nesper, R. *Prog. Solid-State Chem.* **1990**, *20*, 1.
(18) Brewer, L. In *Electronic Structure and Alloy Chemistry of the Transition Elements*; Beck, P. A., Ed.; Interscience Publishers: New York, 1963; p 221.
(19) Hughbanks, T.; Rosenthal, G.; Corbett, J. D. *J. Am. Chem. Soc.* **1988**, *110*, 1511.